

Angular Distributions in

$$B^0 \rightarrow D^{*-} \rho^+ \text{ and } B^+ \rightarrow \overline{D}^{*0} \rho^+$$

CLEO Collaboration

(July 22, 1998)

Abstract

Using 3.1 fb^{-1} of $\Upsilon(4S)$ data (roughly 3×10^6 B pairs) collected with the CLEO detector at the Cornell Electron-positron Storage Ring, we have measured the helicity amplitudes of the decays $B^0 \rightarrow D^{*-} \rho^+$ and $B^+ \rightarrow \overline{D}^{*0} \rho^+$. Our results show the longitudinal polarization in $B^0 \rightarrow D^{*-} \rho^+$ is similar to that $B^0 \rightarrow D^{*-} l^+ \nu_l$ at $q^2 = m_\rho^2$ as expected from factorization. Also there are indications for non-trivial complex phases in helicity amplitudes for both decay modes.

G. Bonvicini,¹ D. Cinabro,¹ R. Greene,¹ L. P. Perera,¹ G. J. Zhou,¹ S. Chan,² G. Eigen,²
 E. Lipeles,² J. S. Miller,² M. Schmidtler,² A. Shapiro,² W. M. Sun,² J. Urheim,²
 A. J. Weinstein,² F. Würthwein,² D. E. Jaffe,³ G. Masek,³ H. P. Paar,³ E. M. Potter,³
 S. Prell,³ V. Sharma,³ D. M. Asner,⁴ J. Gronberg,⁴ T. S. Hill,⁴ D. J. Lange,⁴
 R. J. Morrison,⁴ H. N. Nelson,⁴ T. K. Nelson,⁴ D. Roberts,⁴ B. H. Behrens,⁵ W. T. Ford,⁵
 A. Gritsan,⁵ J. Roy,⁵ J. G. Smith,⁵ J. P. Alexander,⁶ R. Baker,⁶ C. Bebek,⁶ B. E. Berger,⁶
 K. Berkelman,⁶ V. Boisvert,⁶ D. G. Cassel,⁶ D. S. Croccroft,⁶ M. Dickson,⁶
 S. von Dombrowski,⁶ P. S. Drell,⁶ K. M. Ecklund,⁶ R. Ehrlich,⁶ A. D. Foland,⁶
 P. Gaidarev,⁶ R. S. Galik,⁶ L. Gibbons,⁶ B. Gittelmann,⁶ S. W. Gray,⁶ D. L. Hartill,⁶
 B. K. Heltsley,⁶ P. I. Hopman,⁶ J. Kandaswamy,⁶ D. L. Kreinick,⁶ T. Lee,⁶ Y. Liu,⁶
 N. B. Mistry,⁶ C. R. Ng,⁶ E. Nordberg,⁶ M. Ogg,^{6,*} J. R. Patterson,⁶ D. Peterson,⁶
 D. Riley,⁶ A. Soffer,⁶ B. Valant-Spaight,⁶ A. Warburton,⁶ C. Ward,⁶ M. Athanas,⁷
 P. Avery,⁷ C. D. Jones,⁷ M. Lohner,⁷ C. Prescott,⁷ A. I. Rubiera,⁷ J. Yelton,⁷ J. Zheng,⁷
 G. Brandenburg,⁸ R. A. Briere,⁸ A. Ershov,⁸ Y. S. Gao,⁸ D. Y.-J. Kim,⁸ R. Wilson,⁸
 H. Yamamoto,⁸ T. E. Browder,⁹ Y. Li,⁹ J. L. Rodriguez,⁹ S. K. Sahu,⁹ T. Bergfeld,¹⁰
 B. I. Eisenstein,¹⁰ J. Ernst,¹⁰ G. E. Gladding,¹⁰ G. D. Gollin,¹⁰ R. M. Hans,¹⁰ E. Johnson,¹⁰
 I. Karliner,¹⁰ M. A. Marsh,¹⁰ M. Palmer,¹⁰ M. Selen,¹⁰ J. J. Thaler,¹⁰ K. W. Edwards,¹¹
 A. Bellerive,¹² R. Janicek,¹² P. M. Patel,¹² A. J. Sadoff,¹³ R. Ammar,¹⁴ P. Baringer,¹⁴
 A. Bean,¹⁴ D. Besson,¹⁴ D. Coppage,¹⁴ C. Darling,¹⁴ R. Davis,¹⁴ S. Kotov,¹⁴
 I. Kravchenko,¹⁴ N. Kwak,¹⁴ L. Zhou,¹⁴ S. Anderson,¹⁵ Y. Kubota,¹⁵ S. J. Lee,¹⁵
 R. Mahapatra,¹⁵ J. J. O'Neill,¹⁵ R. Poling,¹⁵ T. Riehle,¹⁵ A. Smith,¹⁵ M. S. Alam,¹⁶
 S. B. Athar,¹⁶ Z. Ling,¹⁶ A. H. Mahmood,¹⁶ S. Timm,¹⁶ F. Wappler,¹⁶ A. Anastassov,¹⁷
 J. E. Duboseq,¹⁷ K. K. Gan,¹⁷ T. Hart,¹⁷ K. Honscheid,¹⁷ H. Kagan,¹⁷ R. Kass,¹⁷ J. Lee,¹⁷
 H. Schwarthoff,¹⁷ A. Wolf,¹⁷ M. M. Zoeller,¹⁷ S. J. Richichi,¹⁸ H. Severini,¹⁸ P. Skubic,¹⁸
 A. Undrus,¹⁸ M. Bishai,¹⁹ J. Fast,¹⁹ J. W. Hinson,¹⁹ N. Menon,¹⁹ D. H. Miller,¹⁹
 E. I. Shibata,¹⁹ I. P. J. Shipsey,¹⁹ S. Glenn,²⁰ Y. Kwon,^{20,†} A.L. Lyon,²⁰ S. Roberts,²⁰
 E. H. Thorndike,²⁰ C. P. Jessop,²¹ K. Lingel,²¹ H. Marsiske,²¹ M. L. Perl,²¹ V. Savinov,²¹
 D. Ugolini,²¹ X. Zhou,²¹ T. E. Coan,²² V. Fadeyev,²² I. Korolkov,²² Y. Maravin,²²
 I. Narsky,²² R. Stroynowski,²² J. Ye,²² T. Wlodek,²² M. Artuso,²³ E. Dambasuren,²³
 S. Kopp,²³ G. C. Moneti,²³ R. Mountain,²³ S. Schuh,²³ T. Skwarnicki,²³ S. Stone,²³
 A. Titov,²³ G. Viehhauser,²³ J.C. Wang,²³ J. Bartelt,²⁴ S. E. Csorna,²⁴ K. W. McLean,²⁴
 S. Marka,²⁴ Z. Xu,²⁴ R. Godang,²⁵ K. Kinoshita,²⁵ I. C. Lai,²⁵ P. Pomianowski,²⁵ and
 S. Schrenk²⁵

¹Wayne State University, Detroit, Michigan 48202

²California Institute of Technology, Pasadena, California 91125

³University of California, San Diego, La Jolla, California 92093

⁴University of California, Santa Barbara, California 93106

⁵University of Colorado, Boulder, Colorado 80309-0390

⁶Cornell University, Ithaca, New York 14853

*Permanent address: University of Texas, Austin TX 78712.

†Permanent address: Yonsei University, Seoul 120-749, Korea.

- ⁷University of Florida, Gainesville, Florida 32611
- ⁸Harvard University, Cambridge, Massachusetts 02138
- ⁹University of Hawaii at Manoa, Honolulu, Hawaii 96822
- ¹⁰University of Illinois, Urbana-Champaign, Illinois 61801
- ¹¹Carleton University, Ottawa, Ontario, Canada K1S 5B6
and the Institute of Particle Physics, Canada
- ¹²McGill University, Montréal, Québec, Canada H3A 2T8
and the Institute of Particle Physics, Canada
- ¹³Ithaca College, Ithaca, New York 14850
- ¹⁴University of Kansas, Lawrence, Kansas 66045
- ¹⁵University of Minnesota, Minneapolis, Minnesota 55455
- ¹⁶State University of New York at Albany, Albany, New York 12222
- ¹⁷Ohio State University, Columbus, Ohio 43210
- ¹⁸University of Oklahoma, Norman, Oklahoma 73019
- ¹⁹Purdue University, West Lafayette, Indiana 47907
- ²⁰University of Rochester, Rochester, New York 14627
- ²¹Stanford Linear Accelerator Center, Stanford University, Stanford, California 94309
- ²²Southern Methodist University, Dallas, Texas 75275
- ²³Syracuse University, Syracuse, New York 13244
- ²⁴Vanderbilt University, Nashville, Tennessee 37235
- ²⁵Virginia Polytechnic Institute and State University, Blacksburg, Virginia 24061

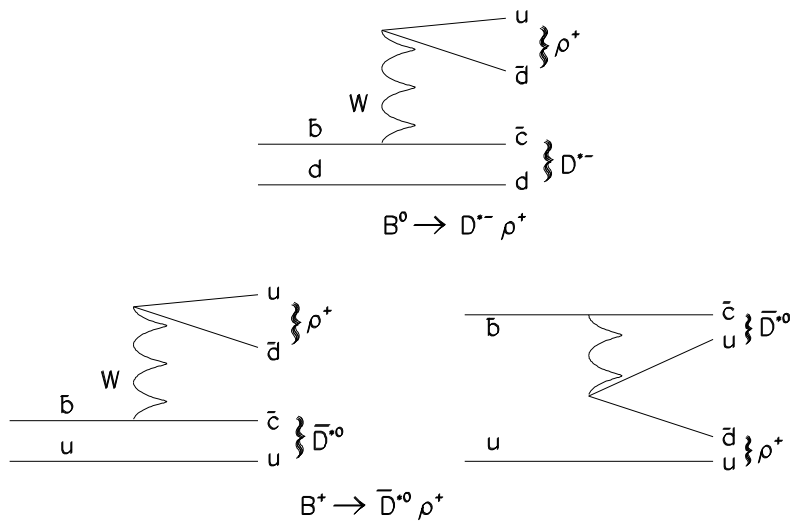


FIG. 1. Feynman diagrams for the decays $B^0 \rightarrow D^{*-} \rho^+$ and $B^+ \rightarrow \bar{D}^0 \rho^+$

I. INTRODUCTION

Hadronic weak decays of heavy flavor meson are complicated by strong interactions which are not exactly solvable. Hard gluon scattering among final states (final state interactions) can significantly modify the decay dynamics. In the factorization approximation it is assumed that the decay matrix element factorizes into a product of two current matrix elements [1], [2]. This is expected to be a good approximation in a two body B decay to a D and a light meson, because the light meson, with a large velocity escapes the interaction region before final state interactions are effective. One sensitive test of this hypothesis is to compare polarization in B meson decay into two vector mesons to a similar semileptonic decay [4]. Since in the semi-leptonic decay there is only one hadronic current, it provides a clean reference to compare with hadronic decays. If the factorization hypothesis is valid one should see similar polarizations in the corresponding hadronic decay. For instance the longitudinal polarization, Γ_L in $B^0 \rightarrow D^- \rho^+$ should be equal to that of $B^0 \rightarrow D^{*+} l^- \nu$ evaluated at $q^2 = m_\rho^2$.

$$\frac{\Gamma_L}{\Gamma}(B^0 \rightarrow D^{*-} \rho^+) = \frac{\Gamma_L}{\Gamma}(B^0 \rightarrow D^{*+} l^- \nu)|_{q^2=m_\rho^2}. \quad (1)$$

In this analysis we study the decay modes $B^0 \rightarrow D^- \rho^+$ and $B^+ \rightarrow \bar{D}^0 \rho^+$ using CLEO II data and look for the presence of final state interactions and the validity of factorization.

Figure 1 shows the Feynman diagrams for the decays. $B^0 \rightarrow D^- \rho^+$ has only an outer spectator contribution, $B^+ \rightarrow \bar{D}^0 \rho^+$ has both outer and inner spectator contributions.

The angular distribution of $B \rightarrow \bar{D}^* \rho$ can be described by three angles (Fig. 2): the polar angle θ_D^* of D^0 in the D^* rest frame, polar angle θ_ρ of π^+ in the ρ^+ rest frame and the angle χ between the decay planes of D^* and ρ^+ in the B rest frame. The final state of the decay is a coherent sum of three possible helicity states where both D^* and ρ can be in helicity 0 states, both in helicity +1 state and both in helicity -1 state. In terms of the angles defined above, the angular distribution is given by

$$\left(\frac{9}{32\pi}\right) |2H_0 \cos \theta_{D^*} \cos \theta_{\rho^-} + H_+ \sin \theta_{D^*} \sin \theta_{\rho^-} e^{i\chi} + H_- \sin \theta_{D^*} \sin \theta_{\rho^-} e^{-i\chi}|^2 \quad (2)$$

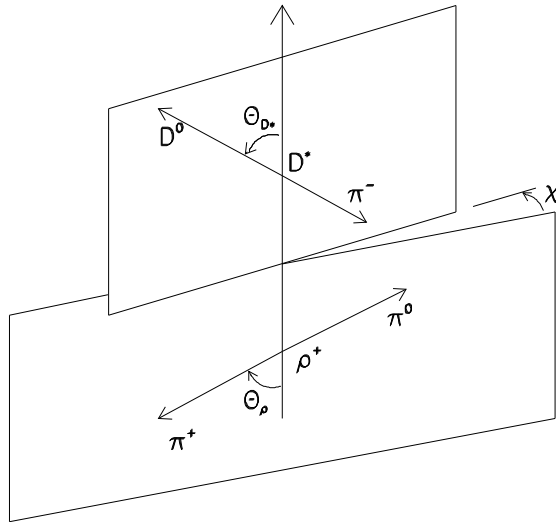


FIG. 2. Definition of decay angles θ_ρ , θ_{D^*} and χ .

where the complex amplitudes H_+ , H_0 and H_- represent the contribution of helicity +1, 0, -1 states. After expanding and rearranging terms

$$\frac{d\Gamma}{d\cos\theta_{D^*}d\cos\theta_\rho d\chi} \propto$$

$$\begin{aligned} & 4|H_0|^2 \cos^2\theta_{D^*} \cos^2\theta_\rho + (|H_-|^2 + |H_+|^2) \sin^2\theta_{D^*} \sin^2\theta_\rho \\ & + 2[\Re(H_+H_-^*) \cos 2\chi - \Im(H_+H_-^*) \sin 2\chi] \sin^2\theta_{D^*} \sin^2\theta_\rho \\ & + [\Re(H_+H_0^* + H_-H_0^*) \cos \chi - \Im(H_+H_0^* - H_-H_0^*) \sin \chi] \sin 2\theta_{D^*} \sin 2\theta_\rho \end{aligned} \quad (3)$$

The normalization

$$\left(\frac{9}{32\pi}\right) \int |2H_0 \cos\theta_{D^*} \cos\theta_{\rho^-} + H_+ \sin\theta_{D^*} \sin\theta_{\rho^-} e^{i\chi} + H_- \sin\theta_{D^*} \sin\theta_{\rho^-} e^{-i\chi}|^2 d\Omega = 1 \quad (4)$$

requires

$$|H_0|^2 + |H_-|^2 + |H_+|^2 = 1 \quad (5)$$

The longitudinal and transverse polarizations are defined by

$$\frac{\Gamma_L}{\Gamma} = \frac{|H_0|^2}{|H_0|^2 + |H_-|^2 + |H_+|^2} \quad (6)$$

and

$$\Gamma_T = \Gamma - \Gamma_L \quad (7)$$

respectively.

Expression 2 is symmetric under $H_\pm \rightarrow H_\mp^*$ so it is not possible to determine which amplitude is the physical H_- or H_+ . Nevertheless for a weak decay we expect H_- to be

larger, so we assign the larger value for H_- in our results. For the \overline{B} decay amplitudes are H_λ^* . Assuming CP conservation

$$H_\pm^* \rightarrow H_\mp \text{ and } H_0^* \rightarrow H_0 \quad (8)$$

this is equivalent to changing χ to $-\chi$ for the anti-particle in Eq. 2. Accordingly we flip the sign of χ for the anti-particle decay in our analysis.

II. EVENT SELECTION

A data sample of 3.1 fb^{-1} integrated luminosity accumulated with the CLEO II detector at the Cornell Electron Storage Ring (CESR), running at center of mass energy at the $\Upsilon(4S)$ resonance. The CLEO II detector is described elsewhere [3]. $B^0 \rightarrow D^{*-} \rho^+$ and $B^+ \rightarrow \overline{D}^{*0} \rho^+$ candidates were found following the decay sequences,

$$\begin{array}{ccc}
 B^0 \rightarrow D^{*-} \rho^+ & & B^+ \rightarrow \overline{D}^{*0} \rho^+ \\
 \downarrow & \searrow & \downarrow \\
 & \pi^+ \pi^0 \rightarrow \gamma\gamma & \pi^+ \pi^0 \rightarrow \gamma\gamma \\
 \downarrow & & \downarrow \\
 \overline{D}^0 \pi^- & & \overline{D}^0 \pi^0 \rightarrow \gamma\gamma \\
 \downarrow & & \downarrow \\
 K^+ \pi^-, K^+ \pi^- \pi^0, K^+ \pi^- \pi^+ \pi^- & & K^+ \pi^-, K^+ \pi^- \pi^0, K^+ \pi^- \pi^+ \pi^-
 \end{array}$$

No cuts were applied for the slow pion from D^{*+} . All other tracks were required to have a momentum above 100 MeV and drift chamber dE/dx was used to identify pions and kaons.

Candidate D^0 s decaying to $K^- \pi^+$, $K^- \pi^+ \pi^0$, and $K^- \pi^+ \pi^- \pi^+$, were required to have their invariant masses respectively within 20 MeV, 25 MeV and 25 MeV of the nominal D^0 mass. Candidate D^{*+} and D^{*0} were reconstructed combining candidate D^0 s with a remaining charged track. Mass difference cuts on candidate D^* and D^0 , $|M(D^0 \pi) - M(D^0) - 142.4| < 1.2 \text{ GeV}$ was applied for both D^{*+} and D^{*0} .

The π^0 candidates were formed by combining two showers whose invariant mass is within 2.5 standard deviations of the nominal π^0 mass. Candidate ρ^+ mesons were selected from $\pi^+ \pi^0$ combinations with invariant mass within 0.15 GeV of the nominal ρ mass of 0.77 GeV.

Reconstructed D^* and ρ^+ were combined to form B candidates. The reconstructed energy of the B candidate was required to be within 50 MeV (60 MeV for $D^0 \rightarrow K^+ \pi^- \pi^0$) of the beam energy. To improve the B mass resolution, the beam constrained mass

$$M_{BC} = \sqrt{E_{beam}^2 - (\vec{p})^2} \quad (9)$$

was calculated constraining the B energy to the beam energy. A cut

$$|\cos \theta_B| < 0.95 \quad (10)$$

was imposed on the polar angle of the B to take advantage of the $\sin^2(\theta_B)$ distribution of the decay of the $\Upsilon(4S)$.

To suppress backgrounds a cut on the cosine of the ‘sphericity angle’ θ_S was applied. The sphericity angle is defined as the angle between the sphericity axis of B and that of the rest

of the event. $|\cos\theta_S| < 0.9, 0.8$ and 0.7 were applied on candidates with D^0 decaying in to $K^-\pi^+$, $K^-\pi^+\pi^0$ and $K^-\pi^+\pi^-\pi^+$ respectively.

About 20% of time there were multiple candidates per event passing the event selection criteria above (mostly coming from misreconstructed ρ^+). In such cases, the candidate with the smallest $|\Delta E|$ was chosen. Figure 3 shows the constrained B mass distributions for the final $\bar{B}^0 \rightarrow D^{*-}\rho^+$ and $B^+ \rightarrow \bar{D}^{*0}\rho^+$ event samples.

III. ANGULAR FIT TO DATA

An unbinned maximum likelihood fit was performed to extract helicity amplitudes from data. The likelihood function \mathcal{L} has the form

$$\mathcal{L} = \frac{e^{-\nu}\nu^n}{n!} \prod_{i=1}^n \mathcal{P}_i \quad (11)$$

where \mathcal{P}_i is the probability of event i occurring, n is the number of events in the data sample and ν number of events estimated by the fit.

The event probability \mathcal{P}_i is

$$\mathcal{P}_i = \frac{S \cdot \epsilon_i \mathcal{P}_{iS} + B \cdot \epsilon_i \mathcal{P}_{iB}}{S + B} \quad (12)$$

S, B are number of signal and background events ($\nu = S + B$), $\mathcal{P}_{iS}, \mathcal{P}_{iB}$ are signal and background probability density functions (p.d.f) which are normalized such that

$$\int \epsilon_i \mathcal{P}_{iS} d \cos \theta_D^* d \cos \theta_\rho d \chi = 1 \quad (13)$$

and

$$\int \epsilon_i \mathcal{P}_{iB} d \cos \theta_D^* d \cos \theta_\rho d \chi = 1 \quad (14)$$

ϵ_i is the detector acceptance which is assumed to be the same for both background and the signal.

The signal probability function, \mathcal{P}_{iS} is assumed to have a Gaussian distribution in B invariant mass, Breit-Wigner shape for ρ and an angular distribution given by Eq. 2. The normalization integral (Eq. 13) was evaluated numerically by summing the signal p.d.f. over signal Monte Carlo events which passed the event selection criteria,

$$\begin{aligned} \int \epsilon_i \mathcal{A}(\theta_{D^*}\theta_\rho\chi) d \cos \theta_{D^*} d \cos \theta_\rho d \chi &= \sum_i^{\text{MC generated}} \epsilon_i(\theta_{D^*}\theta_\rho\chi) \mathcal{A}(\theta_{D^*}\theta_\rho\chi)_{iS} \\ &= \sum_i^{\text{MC accepted}} \mathcal{A}(\theta_{D^*}\theta_\rho\chi)_{iS}. \end{aligned} \quad (15)$$

The background probability is assumed to have a linear shape in B invariant mass in the side band and a quadratic shape under the B signal. The angular distribution of the

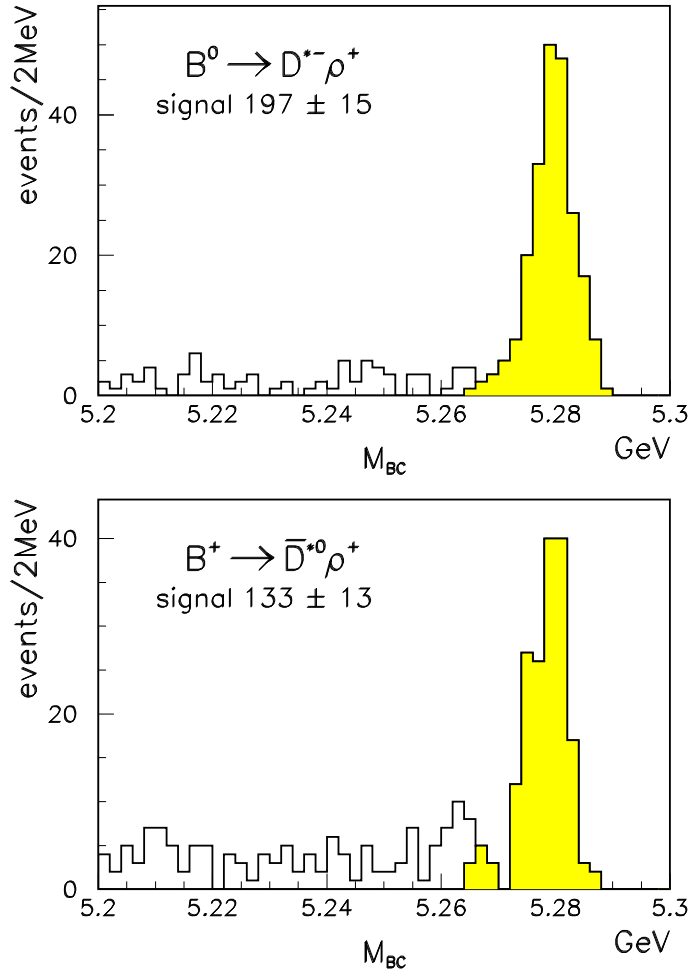


FIG. 3. Beam-constrained mass distributions for $B^0 \rightarrow D^{*-} \rho^+$ and $B^+ \rightarrow \bar{D}^{*0} \rho^+$ candidates. Events are in the shaded region used in the angular fit.

background was taken from a binned fit to the side band events (with invariant mass less than 5.265 GeV). Background p.d.f. normalization was calculated similarly to that of the signal using the same Monte Carlo event sample used to calculate the signal p.d.f. normalization.

The fit minimized:

$$-2 \ln \mathcal{L} = -2 \sum_i^{\text{data events}} \ln \left(\frac{S \cdot \mathcal{P}_{iS} + B \cdot \mathcal{P}_{iB}}{S + B} \right) - 2n \ln \nu + 2\nu \quad (16)$$

where the term $-\sum_i (\ln \epsilon_i - \ln i)$, which is independent of fit parameters and a constant for a given data sample, was ignored. Since only two helicity amplitudes are independent (Eq. 5), the helicity amplitude H_0 was fixed to 1 in the fit and H_- and H_+ (their magnitudes and phases) were measured with respect to H_0 . They were then rescaled to satisfy the normalization condition given by Eq. 5.

IV. FIT RESULTS

Figures 4 and 5 show the projections of the fit on various mass and angular distributions. Results of the fit for helicity amplitudes are given in Table I. The first error is statistical and the second is systematic. Systematic errors include uncertainties due to the background level, angular distribution of the background and smearing effects.¹ Variation due to uncertainty in background angular distribution is dominant (about 60% of the total error) while variation due to smearing is small (about 12%).

The helicity amplitudes correspond to a longitudinal polarization (from Eq. 6) of $87.8 \pm 3.4 \pm 3.0\%$ for $B^0 \rightarrow D^{*-} \rho^+$ and $85.7 \pm 4.7 \pm 4.0\%$ for $B^+ \rightarrow \overline{D}^{*0} \rho^+$

V. CONSISTENCY CHECKS

Several consistency checks were done to verify the fit results.

The ability of the fit to extract correct values was checked by performing the fit on signal Monte Carlo events with known helicity distributions. Monte Carlo event samples used had the same number of events as the data sample. Within errors, the fit gave the correct values.

¹Smearing angular distribution in the signal p.d.f. was assumed to have the form

$$D_{si}(\theta_{D^*}, \theta_\rho, \chi) = \int S(\cos \theta_{D^*}, \cos \theta_\rho, \chi; \cos \theta'_{D^*} \cos \theta'_\rho \chi') \mathcal{A}(\theta'_{D^*} \theta'_\rho \chi') d \cos \theta'_{D^*} d \cos \theta'_\rho d \chi'$$

$S(\theta_{D^*} \theta_\rho \chi, \theta'_{D^*} \theta'_\rho \chi')$ is the smearing function which was approximated by sum of two Gaussians for each of $\cos \theta_{D^*}, \cos \theta_\rho$ and χ distributions.

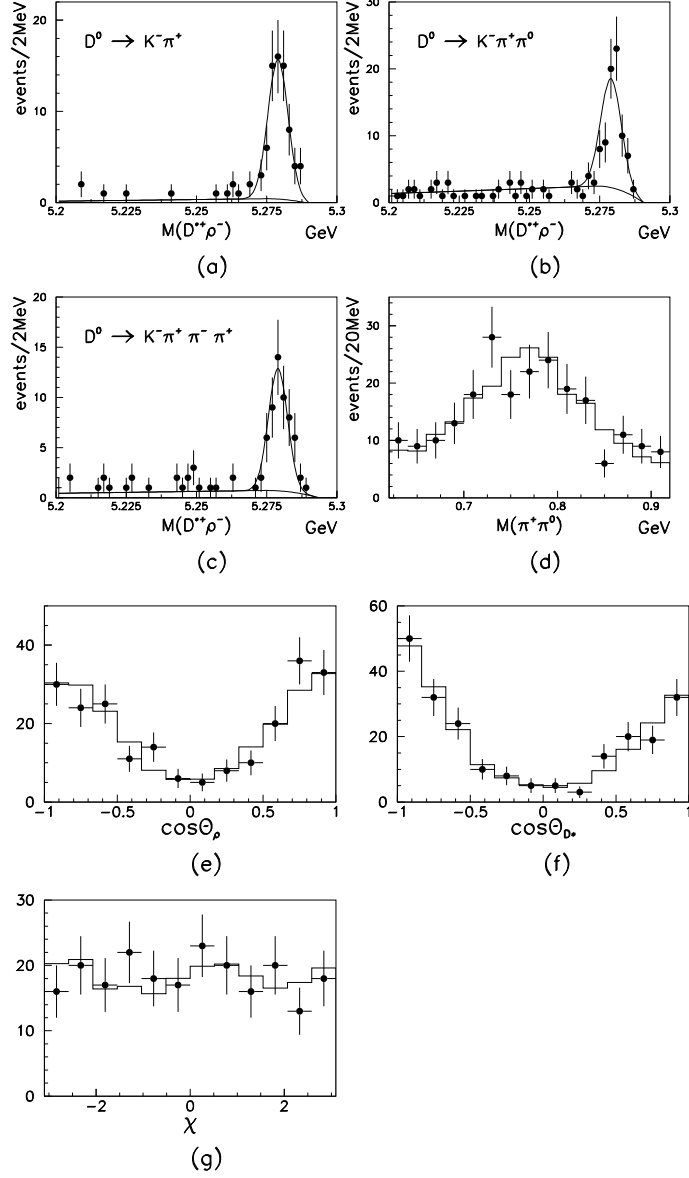


FIG. 4. Fit projections for $B^0 \rightarrow D^{*-} \rho^+$. (a)-(c) fit projection on B invariant mass for events with D^0 decaying in to $K^- \pi^+$, $K^- \pi^+ \pi^0$ and $K^- \pi^+ \pi^- \pi^+$, (d) fit projection on ρ^- invariant mass distribution, (e)-(g) fit projection on $\cos \theta_{D^*}$, $\cos \theta_{\rho}$ and χ . (points: data, histogram/curve: fit projection).

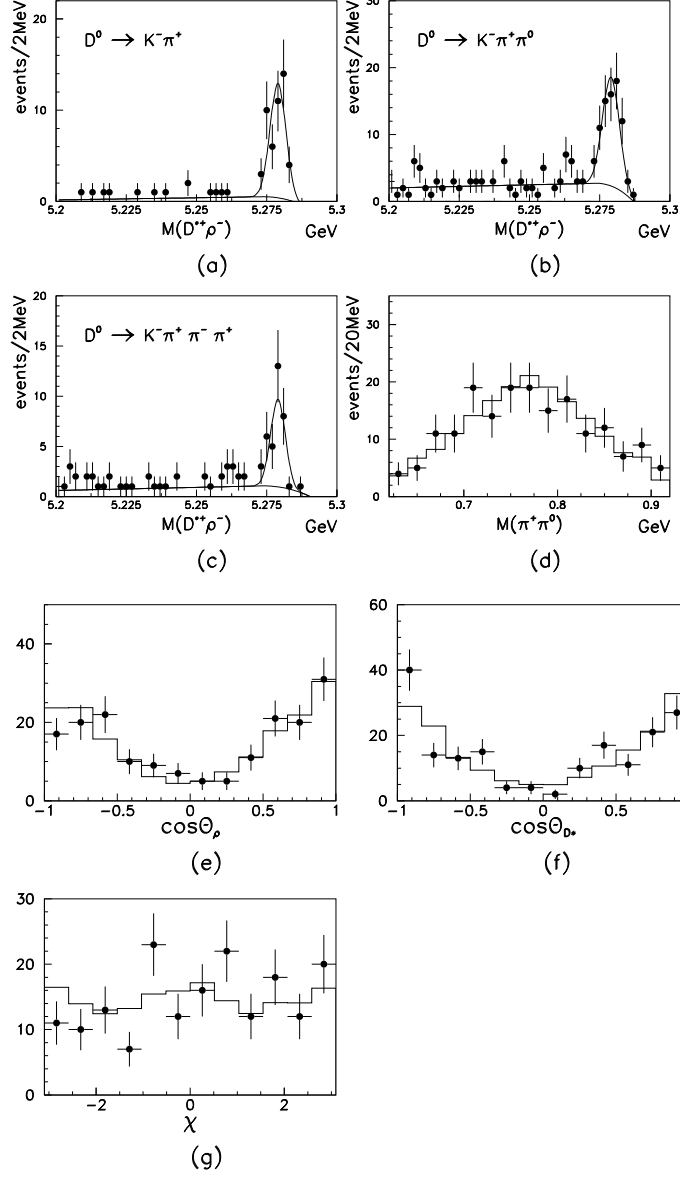


FIG. 5. Fit projections for $B^+ \rightarrow \bar{D}^{*0} \rho^+$. (a)-(c) fit projection on B invariant mass for events with D^0 decaying in to $K^- \pi^+$, $K^- \pi^+ \pi^0$ and $K^- \pi^+ \pi^- \pi^+$, (d) fit projection on ρ^- invariant mass distribution, (e)-(g) fit projection on $\cos \theta_{D^*}$, $\cos \theta_{\rho}$ and χ . (points: data, histogram/curve: fit projection).

	$B^0 \rightarrow D^{*-} \rho^+$		$B^+ \rightarrow \overline{D}^{*0} \rho^+$	
	magnitude	phase	magnitude	phase
H_0	0.936	0	0.932	0
H_-	$0.317 \pm 0.052 \pm 0.013$	$0.19 \pm 0.23 \pm 0.14$	$0.283 \pm 0.068 \pm 0.039$	$1.13 \pm 0.27 \pm 0.17$
H_+	$0.152 \pm 0.058 \pm 0.037$	$1.47 \pm 0.37 \pm 0.32$	$0.228 \pm 0.069 \pm 0.036$	$0.95 \pm 0.31 \pm 0.19$

TABLE I. Fit results for helicity amplitudes. The phase and magnitude of the amplitudes H_+ and H_- are measured with respect to H_0 . In all results first error is statistical and the second error is systematic.

	$B^0 \rightarrow D^{*-} \rho^+$	$B^+ \rightarrow \overline{D}^{*0} \rho^+$
nominal fit $-2 \ln \mathcal{L}$	1363.4	1105.6
zero phase fit $-2 \ln \mathcal{L}$	1369.2	1116.2

TABLE II. Log likelihood values for the nominal fit and for the fit with zero phases

Longitudinal polarization in both decay modes was independently estimated performing binned, one dimensional fits to $\cos \theta_{D^*}$ and $\cos \theta_\rho$ distributions.² Although it does not have the same statistical power as the full fit and does not distinguish signal and backgrounds, it can be used as an approximate check of fit results. Within errors they gave consistent results.

Our fits give non-trivial phases for helicity amplitudes. As is obvious from the second and third lines of the Eq. 3, this should give an asymmetric distribution in the χ distribution of data. χ distributions from our data do not have enough events to show such an asymmetry. However, it is possible to estimate the coefficients involving helicity amplitudes in Eq. 3 by calculating the moments of angular terms. Thus, normalized moments of $\sin \chi \sin 2\theta_{D^*} \sin 2\theta_\rho$ would give the value of $\Im(H_+ H_0^* - H_- H_0^*)$ [5]. Therefore, if one takes the sum of different angular terms over the data sample with a suitable acceptance correction and normalization, all the coefficients in the angular distribution can be estimated. Tables III and IV show the values from the weighted sum compared with values expected from fit results.

Table II shows the fit nominal fit results compared with fits with phases fixed to zero. Fits with zero phases have noticeably worse log likelihood values.

²Integration of Eq. 3 over χ and θ_{rho} results in a angular distribution of the form, $1 + \left(\frac{3P_L-1}{1-P_L} - 1\right) \cos^2 \theta_{D^*}$. P_L is the longitudinal polarization defined by Eq. 6.

ang. term	coefficient	moment	value from fit
$\cos^2 \theta_{D^*} \cos^2 \theta_\rho - \frac{8}{25}$	H_0^2	0.751 ± 0.073	0.859
$\sin^2 \theta_{D^*} \sin^2 \theta_\rho - \frac{12}{25}$	$H_+^2 + H_-^2$	0.159 ± 0.034	0.140 ± 0.040
$\sin \chi \sin 2\theta_{D^*} \sin 2\theta_\rho$	$\Im(H_- H_0^* - H_+ H_0^*)$	0.042 ± 0.103	0.110 ± 0.074
$\cos \chi \sin 2\theta_{D^*} \sin 2\theta_\rho$	$\Re(H_+ H_0^* + H_- H_0^*)$	0.352 ± 0.1044	0.341 ± 0.088
$\sin 2\chi \sin^2 \theta_{D^*} \sin^2 \theta_\rho$	$\Im(H_+ H_-^*)$	0.057 ± 0.024	0.053 ± 0.021
$\cos 2\chi \sin^2 \theta_{D^*} \sin^2 \theta_\rho$	$\Re(H_+ H_-^*)$	0.018 ± 0.023	0.023 ± 0.024

TABLE III. Moments of different angular terms for $B^0 \rightarrow D^{*-} \rho^+$ events compared with values expected from fit results

ang. term	coefficient	moment	value from fit
$\cos^2 \theta_{D^*} \cos^2 \theta_\rho - \frac{8}{25}$	H_0^2	0.626 ± 0.074	0.856
$\sin^2 \theta_{D^*} \sin^2 \theta_\rho - \frac{12}{25}$	$H_+^2 + H_-^2$	0.168 ± 0.036	0.143 ± 0.060
$\sin \chi \sin 2\theta_{D^*} \sin 2\theta_\rho$	$\Im(H_- H_0^* - H_+ H_0^*)$	-0.145 ± 0.101	-0.071 ± 0.109
$\cos \chi \sin 2\theta_{D^*} \sin 2\theta_\rho$	$\Re(H_+ H_0^* + H_- H_0^*)$	0.193 ± 0.109	0.2504 ± 0.105
$\sin 2\chi \sin^2 \theta_{D^*} \sin^2 \theta_\rho$	$\Im(H_+ H_-^*)$	0.002 ± 0.027	-0.011 ± 0.032
$\cos 2\chi \sin^2 \theta_{D^*} \sin^2 \theta_\rho$	$\Re(H_+ H_-^*)$	0.043 ± 0.025	0.068 ± 0.029

TABLE IV. Moments of different angular terms for $B^+ \rightarrow \overline{D}^{*0} \rho^+$ events compared with values expected from fit results

VI. CONCLUSIONS

With unbinned likelihood fits to $B^+ \rightarrow \overline{D}^{*0} \rho^+$ and $B^0 \rightarrow D^{*-} \rho^+$ data we have measured helicity amplitudes of the two decays given in Table I. The slight difference between helicity amplitudes in two modes could be resulting from extra inner spectator contribution in $B^+ \rightarrow \overline{D}^{*0} \rho^+$.

The predicted value of the longitudinal polarization for the semi-leptonic decay $B^0 \rightarrow D^{*-} l^+ \nu$ at $q^2 = m_\rho^2$ is $0.85 - 0.88$ [5 – 8]. The longitudinal polarization at $q^2 = m_\rho^2$ estimated from the CLEO measurement of form factors in $B^0 \rightarrow D^{*-} l^+ \nu$ [9] is $0.914 \pm 0.152 \pm 0.089$. Within errors our measured value of $0.878 \pm 0.034 \pm 0.040$ for the longitudinal polarization in $B^0 \rightarrow D^{*-} \rho^+$ is consistent with those values.

Our likelihood fits indicate non-trivial phases for helicity amplitudes. However, within the statistical power of our data set we were unable to demonstrate this in χ distributions. Non-trivial phases could be due to final state interactions, which can have significant implications for direct CP violation in B decays.

We gratefully acknowledge the effort of the CESR staff in providing us with excellent luminosity and running conditions. This work was supported by the National Science Foundation, the U.S. Department of Energy, Research Corporation, the Natural Sciences and Engineering Research Council of Canada, the A.P. Sloan Foundation, the Swiss National Science Foundation, and the Alexander von Humboldt Stiftung.

REFERENCES

- [1] M. Bauer, B. Stech and M Wirbel, *Z. Phys.* **C 34**, 103 (1987).
- [2] M. Neubert and B Stech, Non-leptonic decays of B mesons, *Heavy Flavors* (Eds. A.J. Buras and M. Lindner) second Edition, World Scientific.
- [3] CLEO Collaboration, Y Kubota *et al.*, *Nucl. Inst. Methods.* **A 320**, 66 (1992).
- [4] J. Korner and G. Goldstein, *Phys. Lett.* **B 89**, 105 (1979).
- [5] A. Dighe, I. Duniez, and R. Fleischer, hep-ph/9804253.
- [6] J. L. Rosner, *Phys. Rev.* **D 42**, 3732 (1990).
- [7] M. Neubert, *Phys. Lett.* **B 264**, 455 (1991).
- [8] G. Kramer *et al.*, *Z. Phys.* **C 55**, 497 (1992).
- [9] J. E. Duboscq *et al.*, *PRL* **76**, 3898 (1996).